8

Electron Microscopy of Liver Biopsies

Theodore C. Iancu and Irena Manov
The Rappaport Faculty of Medicine, Technion-Haifa
Israel

1. Introduction

During the last years of the 20th century, diagnosis in liver pathology was enriched by additional methodologies including immunohistopathology and confocal microscopy. Nevertheless, it soon became obvious that ultrastructural examinations remain essential in both research and diagnosis. The present chapter focuses on the use of electron microscopy in diagnostic hepatology and research of unsolved mechanisms. Attention will be directed to the correct retrieval of specimens for electron-microscopic examination and their processing for obtaining maximal information. The revival of interest in both transmission (TEM) and scanning electron microscopy (SEM) follows continuous changes in the subjects under examination: new diseases or additional features of old diseases; new therapeutic agents and their potentially hepatotoxic effects; environmental factors affecting the liver; identification of viruses and/or other rare noxious agents; immune pathology including liver transplantation and rejection; the liver in systemic-genetic diseases; and ultrastructural pathology in both experimental animals and cell cultures. We herewith wish to provide the clinician (neonatologist, pediatrician, geneticist, and hepatologist-gastroenterologist) with information about the value of electron-microscopic examination *before* performing a liver biopsy and thus enabling him/her to preserve a minute sample for a valuable study.
In his limited size, the present chapter cannot be all-inclusive. Many areas, in which the contribution of electron-microscopy is limited to research investigations, have been left out. Similarly, areas in which histopathology and immune staining are major diagnostic tools, such as in hepatitis, were sidestepped.

2. Technical aspects

Whenever an electron microscopic examination is planned, *immediate fixation of the retrieved specimen is essential*. While most laboratories have their own preference, 2.5% buffered glutaraldehyde is universally accepted. Suggested primary fixative: 2.5% glutaraldehyde in 0.1M sodium Cacodylate buffer (Add 1ml of 25% glutaraldehyde stock to 9 ml of buffer). The specimen should not be larger than 1 mm in each direction to allow for good penetration of the fixative. It is advised to avoid the tip of the cylindrical needle biopsy specimen which may contain sub-capsular liver area and may not be diagnostic. After 2 hrs. (At room temperature or in the refrigerator) continue with the standard steps: osmium post-fixation, dehydration, infiltration, embedding. Do not

freeze at any stage! (For immune-electron microscopy, keep a separate deep-frozen specimen.)
Toluidine blue staining of thick (semi-thin 0.5 μm or 1.0 μm.*) sections for TEM,* used as guideline to the area of interest and further trimming: Reagents: 1% Toluidine Blue and 2% borate in distilled water. *Ultrathin sections,* 40-100 nm (regularly 60 nm for TEM) are spread mostly on 200 or 300 mesh copper grids and stained with uranyl acetate and lead citrate solutions. For iron-containing compounds, keep unstained sections or stained only 2 minutes with lead.
Table I summarizes findings in biopsies of most conditions encountered in clinical cases. The reader can find details in the many books and atlases on hand (Johannessen, 1978; Tanikawa et al., 1979; Ghadially, 1997)).

3. The liver biopsy – general features

Hepatocytes*:* The large, round nuclei usually show an even, round contour and contain 1-2 nucleoli, heterochromatin adjacent to their external border and distinct nuclear membranes and nuclear pores. Uneven, crenated nuclei can follow faulty fixation or other processing problems (Fig. 1). Chromatin margination and fragmentation can indicate apoptosis. In more advanced stages of damage, apoptotic and necrotic cells are seen (Figs. 2-6).

3.1 Damaged and dying liver cells

If the biopsy specimen has been retrieved and fixed correctly, it can be assumed that damaged liver cells indicate a pathological process. The sequences are: edema, swelling of mitochondria, cristolysis, flocculated matrix, nuclear chromatin clumping, margination and fragmentation, (apoptosis), RER denudation, dense deposits in mitochondria, peroxysomes and matrix, necrosis. (Figs. 1-6)

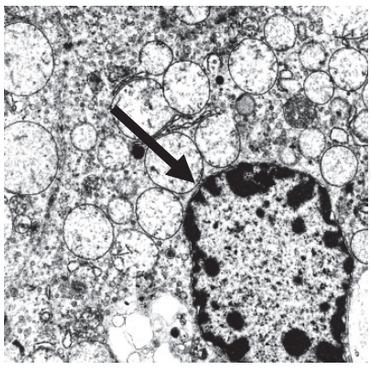

Fig. 1. Delayed fixation: cristolysis and "extracted" matrix of mitochondria; fragmented euchromatin (arrow). x 8,000

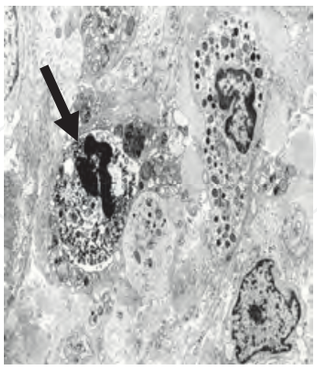

Fig. 2. Necrotic cells in periportal area. Residual necrotic nucleus (arrow). x 5,000

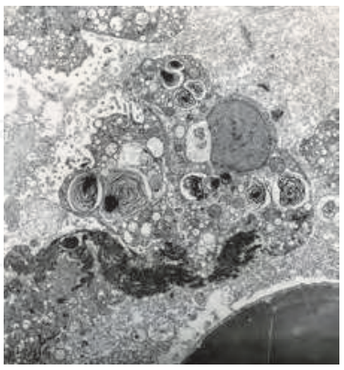

Fig. 3. Disintegrating cell in sinusoid: small nucleus, membraneous lysosomes and some collagen fibers (arrows). x 6,000

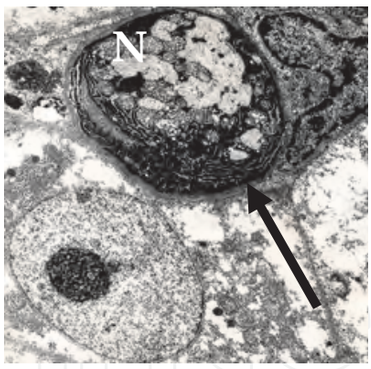

Fig. 4. Apoptotic body: parts of nucleus (N), RER (arrow) and remaining mitochondria in the center. x 6,000

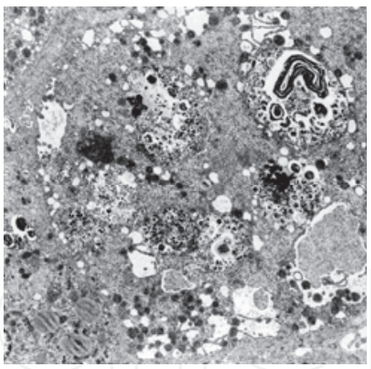

Fig. 5. Extreme biliary necrosis. x 4,000

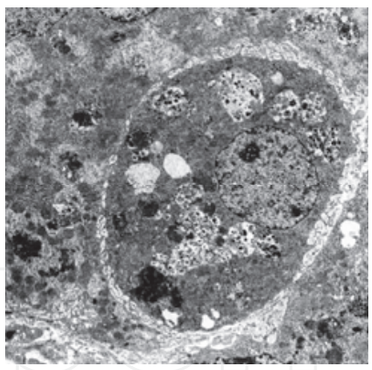

Fig. 6. Biliary necrosis in a detached hepatocyte in the sinusoid. x 5,000

4. Organelle pathology (1): Mitochondria

4.1 Shape and size

Megamitochondria (giant mitochondria, up to 10.0 μm long), existing in numerous metabolic abnormalities including drug reactions and fatty liver; they are frequently elongated along their longitudinal axis. They may contain crystals (Figs. 7, 8), (Sternlieb, 1979). *Amoeboid shape*, found in metabolic abnormalities and Reye syndrome (Partin et al., 1971); *Oncocytic transformation*: mitochondrial crowding similar to an oncocytoma (Tandler et al., 1970) is found generally in hepatocytes in mitochondrial DNA deficiency (Mandel et al., 2001).

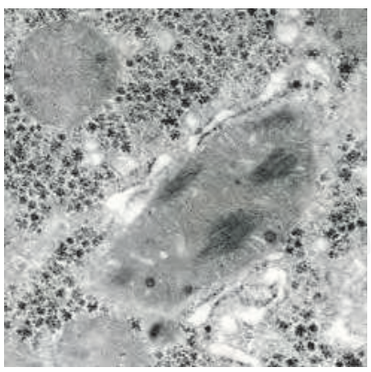

Fig. 7. Fatty liver - NAFLD. Megamitochondrion with longitudinal crystal formations. x 15,000

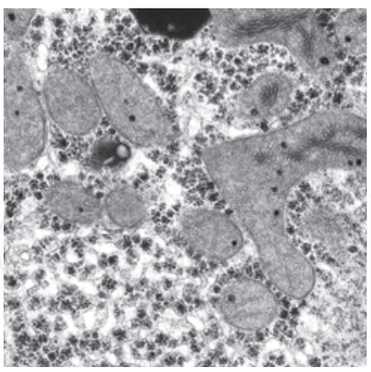

Fig. 8. Lactic acidosis. Angular mitochondrion with twisted and circular cristae. x 15,000

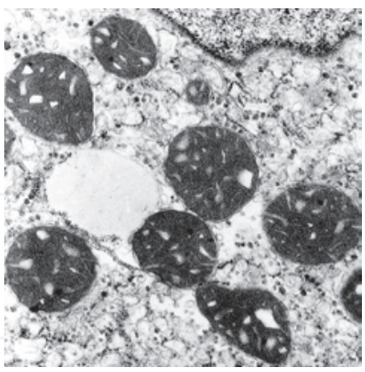

Fig. 9. "Condensed conformation" of mitochondria in "edge artifact". x 8,000

4.2 Content: matrix, cristae, crystals, granules, dense deposits

Orthodox vs. *Condensed* mitochondria. Surrounding conditions induce mitochondrial changes. Mitochondria with dilated cristae and condensed (opaque) matrix are labeled in

'*condensed*' conformation, whereas the apparently 'normal' mitochondria are termed to be in *'orthodox'* conformation (Hackenbrock et al., 1971). Condensed mitochondria are seen at the periphery of a thin section, where *all* cellular components appear more diluted (Fig. 9). We have termed this finding as *edge artifact*. Condensed mitochondria may be seen in pathological conditions (*e.g.* Wilson disease) and thus have diagnostic significance. Therefore we suggest avoiding an *edge artifact* by assessing mitochondria also at safe distance away from the edge.

Cristolysis is a significant, non-specific, sign of mitochondrial injury, when only fragments of cristae remain visible, severed from inner mitochondrial membranes (see Reye syndrome).

Circular or 'curled' cristae are classically seen in cholestasis (Figs. 10, 11); (Phillips et al., 1987); occasionally the cristae are twisted (Figs. 8, 11, 12.). Other variations in amount, position and arrangement remain unexplained, such as: longitudinally stacked; transverse position, perpendicular to the outer membrane; or cartwheel arrangement (Menkes' kinky hair disease) (Ghadially, 1997).

Autolytic changes: specimens retrieved *post mortem* show 'extraction' of matrix and cristae, resulting in empty-looking organelles and nuclei, similar to that of defectively fixed specimens (Fig. 1). *Dense deposits in mitochondria* have been found in Wilson disease (Fig. 13); (Phillips et al., 1987) and in severe iron overload (Bessis & Weed, 1973).

Matrical dense granules, a common, normal feature of mitochondria, are known to contain calcium, but their precise role in mitochondrial function is unknown. However, their generalized absence is an indication of abnormality (drug toxicity, metabolic disturbance?). Large granules may show a hollow center (Fig. 11).

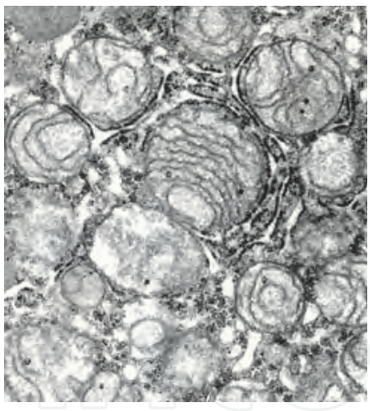

Fig. 10. Circular and stacked cristae in cholestasis. Neonatal hepatitis. x 10,000

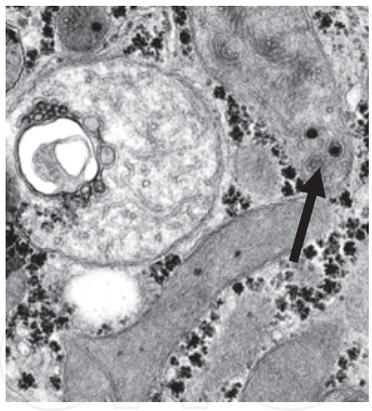

Fig. 11. Metabolic acidosis. Cristolysis and hollow granules (arrow), also in mitochondrion x 15,000

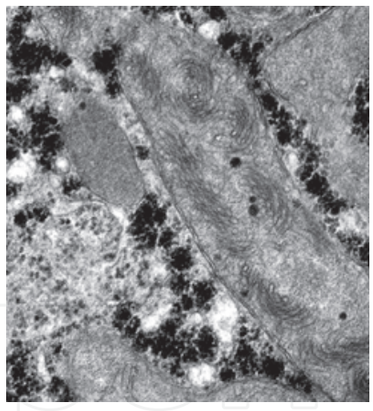

Fig. 12. Metabolic acidosis. Circular and twisted cristae in a mega-mitochondrion. x 20,000

Intramitochondrial inclusions: crystalline, paracrystalline, and filamentous. Crystalline inclusions, have been found in nuclei, cytoplasm and mitochondria (Ghadially, 1997) and show a highly ordered pattern of organization. Crystals with a less ordered arrangement have been named *crystalloid* or *paracrystalline.* The appearance of the crystals depends *'inter alia'* on the plane of sectioning in relationship to the plane of crystal lattice (Figs 7, 14, 15).

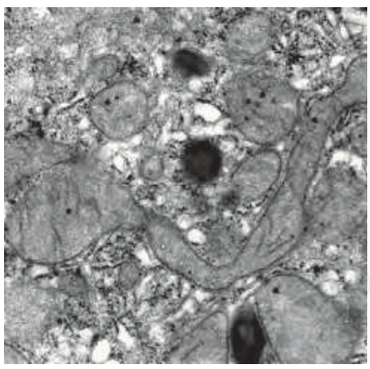

Fig. 13. Wilson disease. Elongated mitochondria and dense deposits. x 15,000.

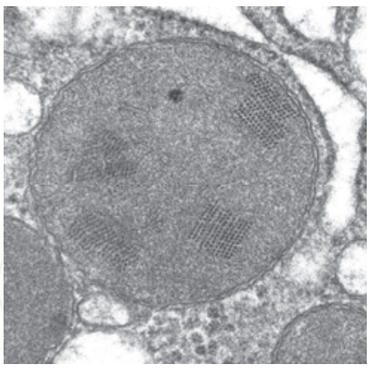

Fig. 14. Aspirin toxicity. Transverse section through paracrystalline formations. x 20,000.

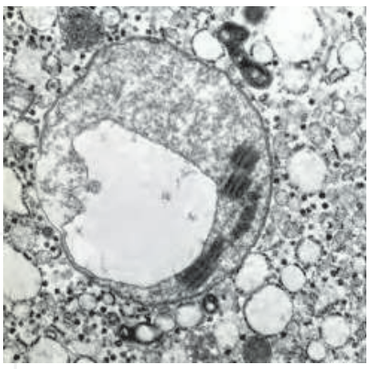

Fig. 15. Aspirin toxicity. Crystalline deposits in giant, abnormal mitochondrion. x 20,000

4.3 Organelle pathology (2): Peroxisomes

Peroxisomes (microbodies) are seen in hepatocytes as round, ellipsoid, slightly angular or elongated organelles. They contain a homogeneous, amorphous, finely granular or flocculent matrix, surrounded by a single tripartite membrane. Randomly distributed in the cytoplasm, they may form clusters. Their diameter is 0.25-1.34 μm and they may exhibit a peripheral terminal or marginal plate of about 0.4 μm long along their limit membrane (Fig. 16). They show variations in number, size, shape and matrix (Fig. 17). The major pathological finding is the absence of peroxisomes in the cerebrohepatorenal syndrome of Zellweger. Conditions with fewer peroxisomes (Table I) comprise *Infantile Refsum disease* (Fig. 18) whereas abundant organelles were reported in Reye syndrome, alcoholic liver disease, clofibrate and 6-mercaptopurine therapy and cholestatic jaundice of pregnancy (Sternlieb, 1979).

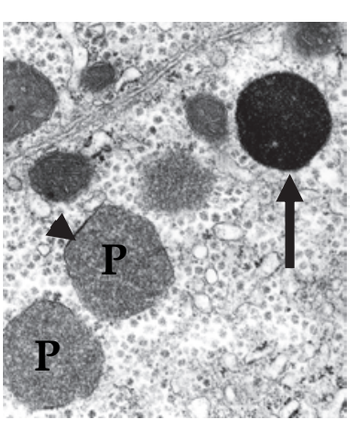

Fig. 16. Siderosome (arrow) *vs.* peroxysomes (P), one with a terminal plate (arrowhead) x 15,000

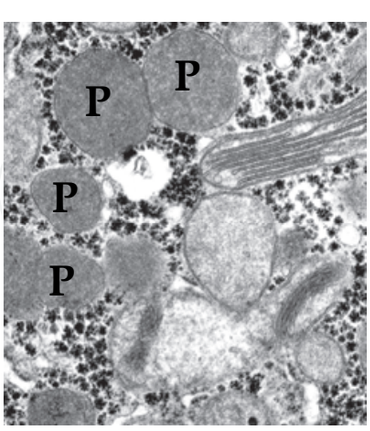

Fig. 17. Metabolic acidosis. Longitudinal arrangement of cristae and multiple large peroxysomes (P). x 15,000

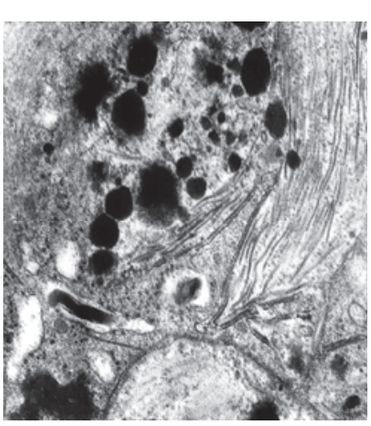

Fig. 18. Infantile Refsum disease, Zellweger variant, absent peroxisomes. Note trilaminar filaments and dense deposits. x 20,000

4.4 Organelle pathology (3): Lysosomes

These Golgi-derived organelles are of major importance in the interpretation of liver biopsies. Their role in autophagy (phagosomes; autophagosomes, autophagolysosomes) and apoptosis has been documented by numerous observations (Ghadially, 1997). In practice, some lysosomes are indicative, if no diagnostic, of *a group of conditions.* Within such a group, further differentiation requires additional (mainly genetic) information. For instance, among storage diseases, identifying a particular mucopolysaccharidosis can be difficult: the lysosomes are *similar,* apparently empty, round or oval single-membrane bound vacuoles (Figs. 19-21.) and may contain a small electron-dense 'nucleoid'. Such appearances have been designated as "the bull's eye" (Fig. 19).

In some cases, the lysosome content discloses the origin of the partially degraded component secluded by autophagy: Glycogen storage disease type II (GSD II, acid maltase or lysosomal alpha–glucosidase deficiency) is typically diagnostic by the presence of modified glycogen molecules (Fig. 22), (McAdams et al., 1974). Siderosomes contain ferritin and/or hemosiderin (Iancu, 1992) and aurosomes and platinosomes the respective metals (Ghadially, 1997); lipolysosomes contain fat droplets (Hayashi & Sternlieb, 1975); Experiments with Thorotrast and carbon particles have demonstrated the phagocytic capacities of lysosomes (Ghadially, 1997).

5. Inborn lysosomal and metabolic diseases

5.1 Lysosomal diseases

The established criteria for this group of conditions have been postulated by Hers (Hers, 1963) as follows: "genetic deficiency of one of the acid hydrolases that is normally localized within the lysosome; consequent accumulation of undigested material within single-membrane-bound organelles that are altered lysosomes". The classical example of lysosomal storage disease, GSD II is due to lysosomal alpha-glucosidase deficiency, an enzyme encoded in humans by the *GAA* gene.

Lysosomal storage disorders have been listed in numerous publications and recently by Pastores (Pastores, 2010). This classification, as well as the present Table I, is based on the relevant substrate involved. We have selected previously unpublished electron micrographs to exemplify diagnostic features.

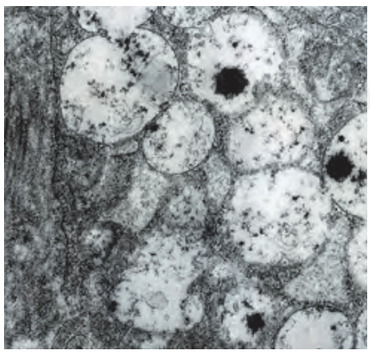

Fig. 19. "Bull's eye" appearance of nucleoid-containing lysosomes in mucopolyscaccharidoses. (Hurler). x 15,000

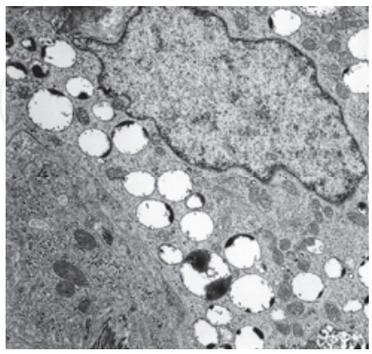

Fig. 20. Sinusoidal cell: Mucopolysaccharidosis (Hunter). Note typical lysosomes. x 6,000

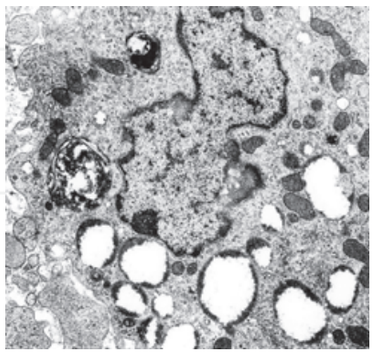

Fig. 21. Mucopoly-saccharidosis. "Empty looking" lysosomes and degraded phagolysosomes. (Morquio). x 6,000

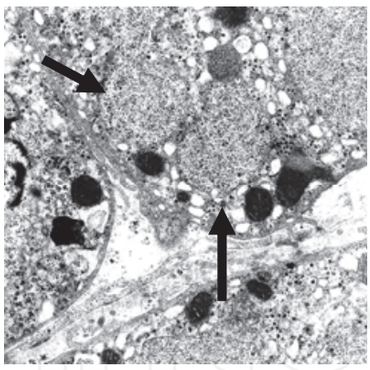

Fig. 22. Acid maltase deficiency (Pompe). Monoparticulate glycogen in membrane-limited bodies (arrows). x 10,000

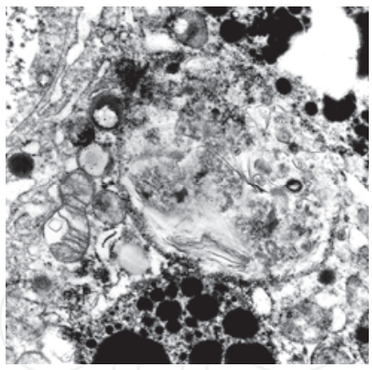

Fig. 23. GM1 Gangliosidosis (Landing). Filaments in a large lysosome; dense deposits, possibly related to TPN. x 10,000

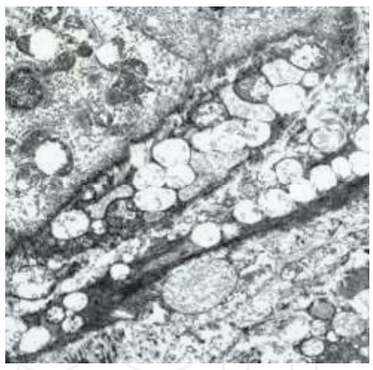

Fig. 24. Sialidosis: numerous single-membrane limited lysosomes in a sinusoid. x 5,000

5.1.1 Mucopolysaccharidoses (MPS)

This group includes diseases with intralysosomal storage and urinary excretion of partially degraded mucopolysaccharides. By TEM, single-membrane-bound bodies show scarce flocculent and particulate precipitate lying in a lucent matrix in many tissues (Tondeur and Neufeld, 1975). They are found in various diseases of the group (see Table 1), with only minor differences (Figs. 19-21). Of interest is the presence of a "nucleoid", remnant after extraction by processing of lysosomal content (Fig. 19). The appearance of several other conditions with empty-looking lysosomes and occasional electron-dense deposits may generate diagnostic difficulties, *e.g.* gangliosidosis (Fig. 23) sialidosis (Fig. 24), fucosidosis, mannosidosis.

5.1.2 Gaucher disease (GD)

The most prevalent lysosomal storage disease, GD is due to a deficiency of glucocerebrosidase leading to accumulation of glucosylceramide in "Gaucher cells", in the liver and other organs. These cells can be found in other conditions (*pseudo*-Gaucher cells) but characteristically in the three forms of GD: Type I-chronic non-neuropathic, (90% in Ashkenazi Jews); Type II (acute neuropathic); and Type III (subacute neuropathic). Bone marrow or liver biopsy examinations for diagnosis have been replaced by glucocerebrosidase determination in leukocytes or cultured fibroblasts, or by mutation analysis. Liver biopsy is reserved for *hydrops fetalis* in congenital GD or unclear cases of hepatosplenomegaly. The pale-staining cytoplasm of the large, multinucleated Gaucher cells, show by TEM large lysosomes containing long tubules, some twisted and intermingled (Fig. 25). (Chakrapani & Green, 2004)

5.1.3 Niemann–Pick Disease (NPD) including type A (NPA), B (NPB) and C (NPC)

NPDs of various types can begin as fetal disease or neonatal jaundice. Some types and mutants can show relatively late-onset hepatosplenomegaly. The histopathological characteristic of this group of storage diseases is the presence of "foamy cells" storing sphyngomyelin. While diagnosis of NPA and NPB is by sphingomyelinase assays and mutation analysis, NPC1 need be diagnosed by mutational analysis at the level of cDNA

and/or assaying cultured fibroblasts for cholesterol esterification and staining for unesterified cholesterol with filipin (Meiner et al., 2001). The advantage of TEM over these methods is that it can provide a more rapid diagnostic confirmation by identifying suspicious cells, usually liver or amniotic cells (Fig. 26), (Spiegel et al., 2009).

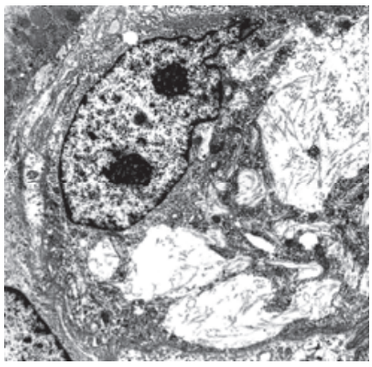

Fig. 25. Part of Gaucher cell showing typical fibrils. x 10,000

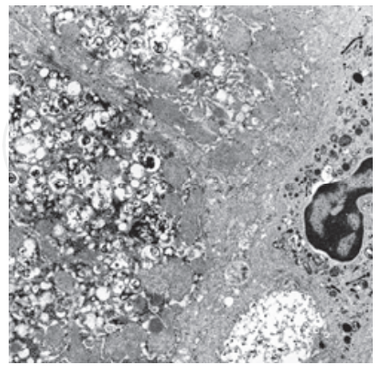

Fig. 26. Niemann-Pick C: membranous whorls fill hepatocytes. x 4,000

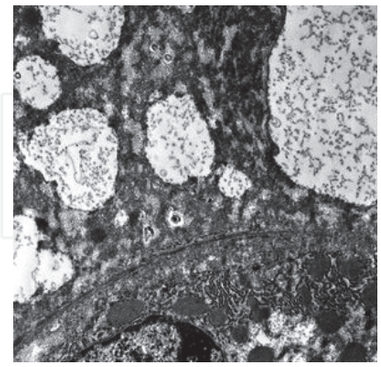

Fig. 27. "Fructose holes" in hereditary fructose intolerance. x 6,000

5.2 Cholestasis

Cholestasis**,** appearing in conditions in which the bile flow is blocked, is still differentiated as extra-hepatic- and intra-hepatic. There are only few differential features revealed by electron microscopy.

Pre-and post-natal bile-production and secretion may be hindered by morphological and functional abnormalities. Neonatologists are more troubled by jaundice associated to *direct-binding (conjugated) bilirubin* frequently indicating the possibility of structural abnormalities, such as *biliary atresia*. Liver biopsy is usually required to confirm this life-saving surgical correction. Other conditions associated with conjugated bilirubin are listed in Table 1 and several reviews (Balistreri, 2002); Suchy, 2004). Meanwhile, new clinical, morphological and genetic characteristics continue to emerge (Bull et al., 1997; Bezerra & Balistreri, 1999; Davit-Spraul et al., 2009). Other conditions, in which basic conditions are associated with cholestasis, are listed for differential diagnosis (Roberts, 2004 a).

5.2.1 Ultrastructural features of cholestasis

Hepatocytic mitochondria show circular, concentric or curled cristae (Fig. 10, 28). With continuing cholestasis, bile-containing bodies are seen as clusters, mostly around bile canaliculi. In their outer limit, a membranous structure is occasionally identified. The bile-containing bodies, considered lysosomes, are electron-opaque organelles, usually 0.5-2.0 (0.1-10.0) μm diameter (Fig. 29). Bile canaliculi display distension and damaged microvilli (Fig. 30). In time, spicular conglomerates become visible (Fig. 31). Myelin-like membranes are noticeable in long-standing cholestasis (Fig. 32).

Bile leakage into the cytosol (amorphous, without limit membrane) appears after prolonged, severe cholestasis. Cells other than hepatocytes (Kupffer cells, sinusoidal lining cells, stellate cells, bile duct epithelia) exhibit variable degrees of cholestasis, mainly as bile-containing lysosomes. *Focal biliary cytoplasmic necrosis* is the extreme form of bile-induced hepatocytic damage, other than biliary cirrhosis (Fig. 33).

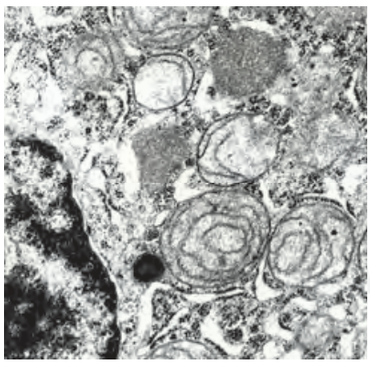

Fig. 28. Hepatocyte. Circular and curled cristae in cholestasis. Peroxysomes (P). x 8,000

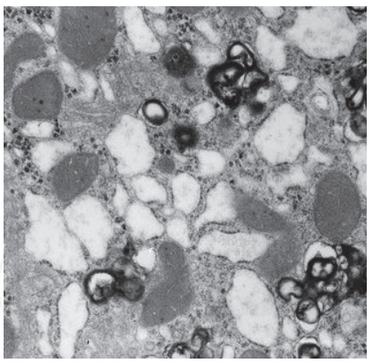

Fig. 29. Bile-containing lysosomes in the pericanalicular area. Note dilated RER. x 4,000

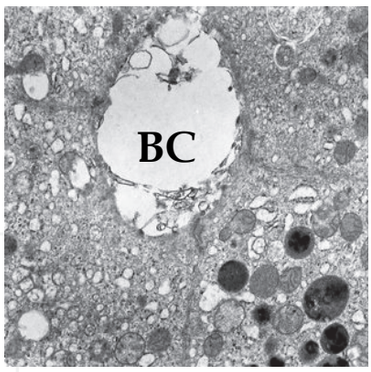

Fig. 30. Distension of canaliculus (BC) and loss of microvilli in cholestasis. x 4,000

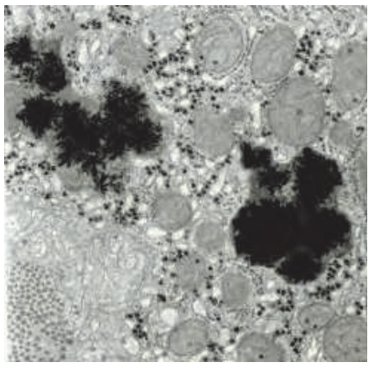

Fig. 31. Severe cholestasis: spicular bile x 10,000

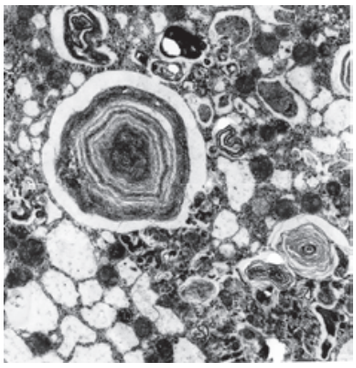

Fig 32. Myelin-like lysosomes in a degraded hepatocyte. x 8,000

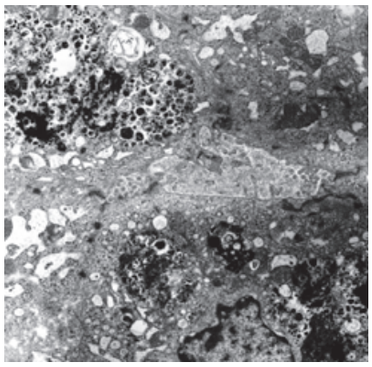

Fig. 33. Focal biliary cytoplasmic necrosis, near bile canaliculi. x 4,000

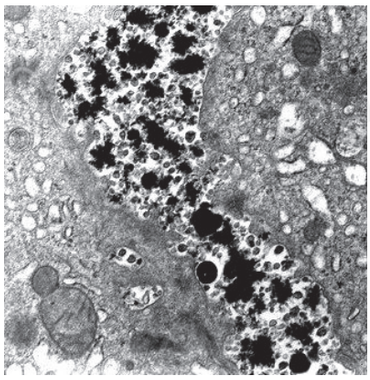

Fig. 34. Cholestatic jaundice. "Byler-like" bile in PFIC-1. x 6,000

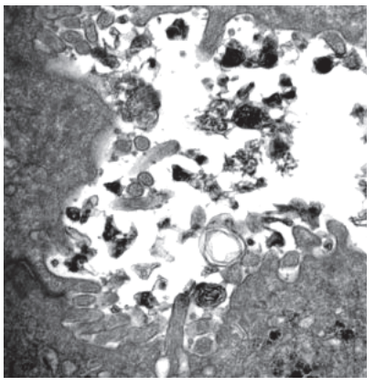

Fig. 35. PFIC-1. "Byler-like" bile. Distended canaliculus, injured microvilli. X 4,000

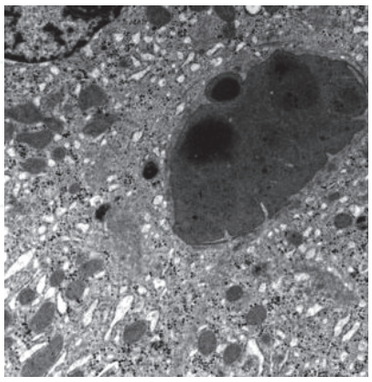

Fig. 36. Bile plug in biliary atresia. x 4,000

5.2.2 PFIC-1, PFIC-2 and PFIC-3

PFIC-1 (former Byler disease) is caused by a mutation in the *ATP8B1* gene on chromosome 18q21-22. Byler-like bile, seen in PFIC-1, is formed of coarse granular bile in distended canaliculi with damaged/absent microvilli (Figs. 34-35). In contrast, the bile in PFIC-2 is not granular but filamentous, important for differential diagnosis. Bile plugs are typically seen in severe obstructive cholangiopathies including biliary atresia (Fig. 36).

PFIC-2 is caused by a mutation in the *ABCB11* gene on chromosome 2q24 that encodes the bile salt export pump (BSEP). BSEP is the major canalicular bile acid pump, and thus the loss of BSEP function results in severe hepatocellular cholestasis. Both PFIC-1 and PFIC-2 are characterized by low gamma-glutamyl peptidase (GGT) levels. Although genetically distinct, PFIC1 and PFIC2 are both caused by the absence of a gene product required for canalicular export and bile formation. Clinically and histologically there are few differences between these conditions, which may both advance to cirrhosis. An important contribution of electron microscopy to the otherwise ample description of histopathological features of PFIC, is the finding of the coarsely granular "*Byler bile*" in dilated canaliculi that lack microvilli and are cuffed by a thick layer of microfilaments. "Byler bile", is apparently related to the defect in canalicular bile acid transport with primary retention of hydrophobic bile salts. Weber suggested the microfilament collar was a feature of cholestasis in another ethnic group (Weber et al., 1981). Bull and co-authors reported that "Byler bile" was found only in children who were homozygous for the microsatellite haplotype at 18q21-q22 (PFIC 1)(Bull et al., 1997). It should be noted that Byler bile can be seen occasionally in cholestatic conditions other than PFIC 1 or PFIC 2, such as Familial Progressive benign cholestasis (Phillips et al., 1987).

The absence of bile salts in the bile ducts in PFIC1 and PFIC2 and their presence in the bile ducts in PFIC3 accounts for the difference in biochemical tests. In PFIC3, as in most cholestatic diseases, exposure of duct cell membranes to bile salts results in solubilization of GGT, absorption of the enzyme into the circulation, and elevated serum GGT levels. In contrast, in PFIC1 and PFIC2 there are low levels of bile salts, the GGT is never solubilized, and the serum GGT is normal. Rather than defective bile acid export, patients with PFIC3 have deficient hepatocellular phospholipid export. The lack of phospholipids produces destabilized micelles and promotes lithogenic bile with crystallized cholesterol which could produce small bile duct obstruction (Davit-Spraul et al., 2009). The histological and ultrastructural features are similar to other forms of PFIC, except for the absence of Byler bile. In PFIC-3 the bile is amorphous or filamentous. The patients become symptomatic at various ages, from 1 month to 20 years, and progression to cirrhosis can be rapid (first decade).

Recently (Verhulst et al.), 2010), reported on the critical role of ATP8B1 (deficient in PFIC-1) in apical membrane organization, potentially relevant for development of cholestasis and extrahepatic manifestations associated with ATB8B1 deficiency (such as disorganized apical actin cytoskeleton and defective microvilli formation)

5.2.3 Crigler-Najjar

This syndrome is divided into two types: type I and type II, with the latter sometimes called Arias syndrome. These two types, along with *Gilbert's syndrome, Dubin-Johnson syndrome,* and *Rotor syndrome,* make up the five known *hereditary defects in bilirubin metabolism.* Unlike Gilbert's syndrome, only a few hundred cases of Crigler-Najjar syndrome are known to exist (Kelly, 2004).

5.2.4 Dubin-Johnson syndrome

Originally termed canalicular multiple organic anion transporter (cMOAT) defect, it is also known as *multidrug resistance protein 2 (MRP2*) and is a member of the *ABC transporter superfamily*. The gene that encodes the transporter is *ABCC2* is found on chromosome 10. Rare cases of neonatal hepatitis have been reported; in older children, histology and TEM show typical melanin-containing pigment predominantly in the centrilobular area, around bile canaliculi (Fig. 37).

5.2.5 Alagille syndrome (Arteriohepatic dysplasia)

Described in 1975, the syndrome comprises infantile cholestasis, hepatic ductular hypoplasia, typical facies, peripheral pulmonic stenosis, vertebral anomalies and physical and mental retardation. The persistence of cholestasis is not associated to extra-hepatic obstruction but paucity of intralobular bile ducts is frequent. Valencia-Mayoral et al. have found ultrastructural changes suggesting a block in the Golgi apparatus or in the pericanalicular cytoplasm (Valencia-Mayoral et al., 1984). These TEM findings in Alagille syndrome appear to be distinctive when compared to other cholestatic syndromes.

5.2.6 Alpha-1-antitrypsyn deficiency (A1AT)

This disorder is a relatively common autosomal co-dominant condition causing chronic lung and liver disease. α_1-antitrypsin is a protease inhibitor belonging to the *serpin superfamily*. It is generally known as serum trypsin inhibitor. A point-mutation induces aggregation-prone properties to a secretory protein so that the retained mutant protein is not secreted into blood or body fluids. Accumulation of the mutant A1AT in the RER of hepatocytes, typically seen with the TEM (Fig. 38) causes liver inflammation and carcinogenesis by a gain-of-toxic function mechanism. Studies performed over the last years have shown the importance of autophagy in disposal of mutant, a phenomenon also demonstrated by TEM. In infancy, A1AT is an important cause of cholestatic jaundice, with giant cell hepatitis, mimicking biliary atresia and Alagille syndrome (Mowat, 1994).

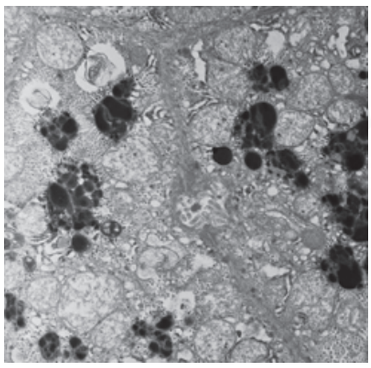

Fig. 37. Dubin-Johnson syndrome. Electron-dense accumulations adjacent to bile canaliculus. x 5,000

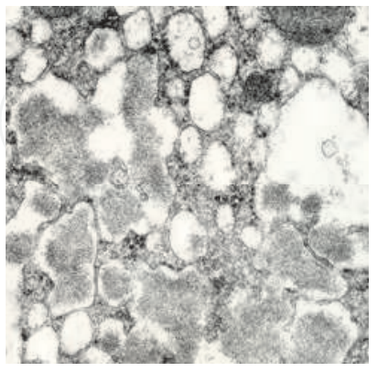

Fig. 38. Alpha-1-antitrypsin deficiency: amorphous accumulations in RER. x 6,000

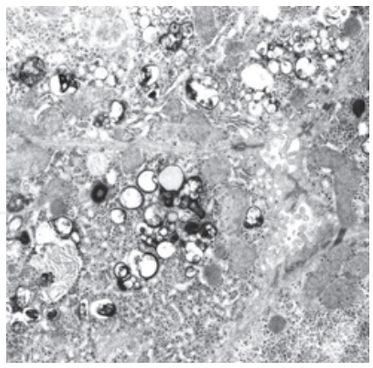

Fig. 39. Congenital disorder of glycosylation (CDG). Pericanalicular clusters of single-membrane-bound bodies. x 5,000

5.3 Congenital disorders of glycosylation (CDG)

This new group of genetic diseases characterized by defective glycoprotein biosynthesis exemplifies the value of electron microscopic diagnosis by liver biopsy (Iancu et al., 2007) The patients can present either with a neurological form (psychomotor retardation, cerebellar hypoplasia and retinitis pigmentosa, or with a multivisceral form with neurological and extra-neurological manifestation including liver, cardiac, renal or gastrointestinal involvement). A form with liver involvement and/or cardiomyopathy, enteropathy and hypoglycemia has also been reported. Elevated transaminases may focus attention to the liver. The biopsy shows increased cellularity, distorted bile ducts and small- and medium size lipid droplet steatosis. TEM shows, in addition, the presence of numerous myelinosomes. These organelles are mainly empty whorls measuring 0.02-0.1 μm and forming conglomerates ("grape-like") close to bile canaliculi (Fig. 39). Isoelectric focusing of transferrin provides an easy method of identification of CDG's.

5.4 Galactosemia, fructose intolerance, tyrosinemia

These inherited metabolic disorders are included here because of their common presentation with jaundice and elevated transaminases, as evidence of liver involvement. Although TEM results are not always specific, if a biopsy is performed, the findings can be supportive for life-saving diagnosis (Phillips et al., 1987; Mowat, 1994).

*Galactosemia: e*nlarged hepatocytes, dilated RER, fatty liver, focal cytoplasmic degeneration, biliary necrosis;

Hereditary fructose intolerance: punched-out cytoplasmic lysis - "fructose holes" (Fig. 27).

Tyrosinemia: Increased lipid, dilated RER, pleomorphic mitochondria and focal necrosis.

5.5 Siderosis

Inorganic iron is revealed by TEM in *unstained* or slightly stained sections. The compounds are electron-dense due to the presence of *ferritin* and/or *hemosiderin* (Iancu, 1983; Iancu, 1992) and (rarely) *iron-containing micelles* (Fig. 40), (Bessis & Weed, 1973; Iancu, 1983; Iancu, 1992). The octahedral storage molecule ferritin (Holoferritin = ferritin core (Fe hydroxyphosphate) + apoferritin protein coat) becomes visible by TEM when the core contains more than about 1,500 inorganic iron molecules, up to a maximum of 4,500 molecules (*iron-rich ferritin).* Ferritin molecules (cores) can be seen randomly dispersed within the cell sap of hepatocytes, sinusoidal and Kupffer cells (Fig. 41, 42) in amounts depending on the origin of overload (absorptional or transfusional). The accumulation of iron is easier detectable in *lysosomes.* Iron-containing lysosomes are termed *siderosomes.* They contain electron-dense iron in 3 forms: a) ferritin molecules (mostly iron-rich variety), frequently associated with pseudo-membranous layers and forming arrays or hexagonal crystals; b) coalesced ferritin particles (after degradation of their apoferritin coat) forming 'clumps' of hemosiderin with extreme electron-density; c) siderosomes in which smaller particles can be resolved, apparently an intermediate stage between a) and b). Yet, a strict electron-microscopic definition of these compounds emphasizes that *hemosiderin* is formed when the coat of apoferritin is smaller than 0.25 nm and thus the distance between two ferritin molecules is reduced to less than 0.5 nm (Fischbach et al., 1971)

The TEM study of liver siderosis reveals: presence of ferritin and/or hemosiderin within various cells; relationship with additional conditions (e.g. cirrhosis, hepatitis, and carcinoma); quantification of the iron-containing compound by mass spectrometry or other analytical methods; and assessment of putative effect of a chelating agent. TEM confirmed that iron

overload from excessive absorption (hemochromatosis HFE) produces parenchymal overload with an initial mild reticuloendothelial (RES) overload, while transfusional iron is located mostly in the RES, followed by re-distribution of excess iron among both compartments.

5.5.1 Genetic hemochromatosis (HFE) "classical" hemochromatosis, type 1

Hemochromatosis HFE is most often caused by a mutation in the gene HFE on chromosome 6p21.3. Four types were identified (Muir et al., 1984), with differences between the degrees of liver iron loading. Children as young as 4 years had juvenile forms. The various stages of overload were followed by TEM (Iancu et al., 1997).

5.5.2 Other iron-loading conditions

In homozygous β-thalassemia, excess iron originates from hemolysis, increased absorption and frequent blood transfusions. In the liver, "foreign "transfused iron is channeled to the (RES), whereas iron from excessive absorption reaches parenchymal cells. The end-result is severe overload possibly followed by cirrhosis and/or hepatocellular carcinoma. In aplastic anemia and dialysis, iron derives from transfusions, with predominant initial RES overload, followed by redistribution towards hepatocytes and aggravation of liver siderosis as seen at the ultrastructural level. (Iancu, 1989; Iancu, 2011).

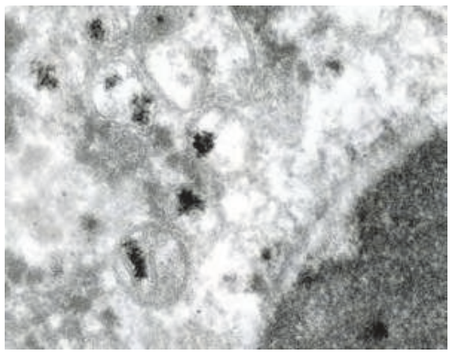

Fig. 40. Homozygous beta-thalassemia: Electron-dense iron micelles within mitochondria. x 20,000, unstained

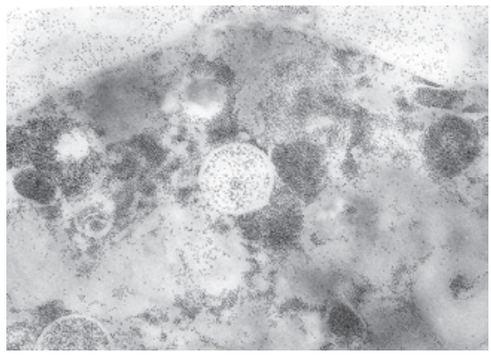

Fig. 41. Genetic hemochromatosis HFE. Ferritin cores in a Kupffer cell, dispersed and/or aggregated. x 20,000, unstained

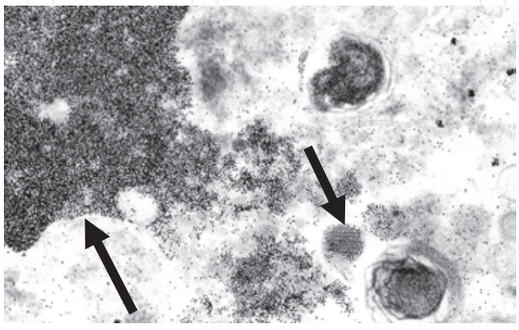

Fig. 42. Hepatocyte from β-thalassemia major. Ferritin dispersed or coalesced in crystals (curved arrow). In hemosiderin, (arrows) ferritin particles cannot be resolved anymore. x 20,000, unstained

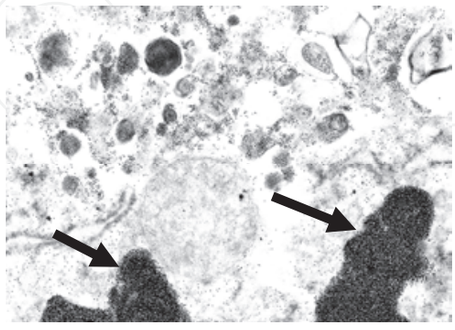

Fig. 43. Neonatal hemochromatosis, similar to genetic hemochromatosis: note ferritin of variable electron-density ("iron-rich" *vs.* "iron-poor") and hemosiderin "clumps" (arrows). x 20,000, unstained.

5.5.3 Neonatal hemochromatosis (NH)

In the neonatal period, the liver normally contains relatively large amounts of ferritin and hemosiderin, which diminish during the first year of life.

Neonatal hemochromatosis is a severe, frequently fatal condition. It has been found in fetuses and newly born infants presenting with rapidly progressing liver failure. The pattern of liver siderosis is similar to that of hereditary hemochromatosis (HFE) but the pace of pathological changes is fulminant: there is a striking difference between the iron-loaded hepatocytes and the sinusoidal cells which show only minor iron deposition. Perls' stain reveals siderosis in extra-hepatic locations (pancreas, thyroid, heart). Until recently, the cause and mechanism of this condition were unknown. Presently, NH is considered an alloimmune disease in which maternal antibodies damage the hepatocytes, especially post-partum. The siderosis is seen as secondary to the damaged liver cells and not the primary metabolic abnormality (Knisely & Vergani, ; Whitington, 2007). Because of the life-endangering condition of these infants, liver biopsy is rarely performed. TEM reveals iron mainly in hepatocytes, stored similarly to other parenchymal loading disorders (Fig. 43).

The role of iron in the brain and in Parkinson and Alzheimer diseases is under continuous study. Iron-induced lipid peroxidation and the formation of toxic free radicals appear to contribute to the development of the latter conditions (Zhu et al., 2007). Ongoing experimental work is focused on the effect of new chelating agents, capable to pass the blood-brain-barrier (Gal et al., 2006) and reduce the damaging effects of iron. Using cultured hepatoma-derived Hep3B cells loaded with inorganic iron, we could demonstrate the effect of a new bimodal chelator M30 capable of reducing ferritin in these cells, as seen by immunofluorescence (personal communications, Y Bashenko, 2009-2011).

5.5.4 Wilson disease (WD)

In this copper metabolism abnormality, there are numerous ultrastructural changes in liver cells as the liver lesions change in time, from chronic hepatitis to acute liver failure or cirrhosis. Alterations involve nuclei, mitochondria, peroxisomes, RER, fatty changes with lipolysosomes and neocholangioles with copper deposits (Figs. 44-47) (Sternlieb, 1979) Phillips et al., 1987).

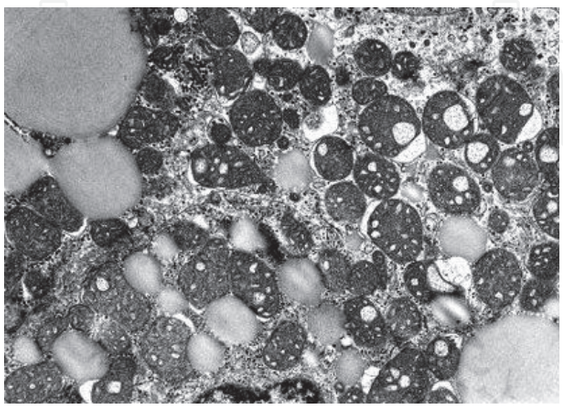

Fig. 44. Punched-out mitochondria and fat droplets in WD. x 6,000

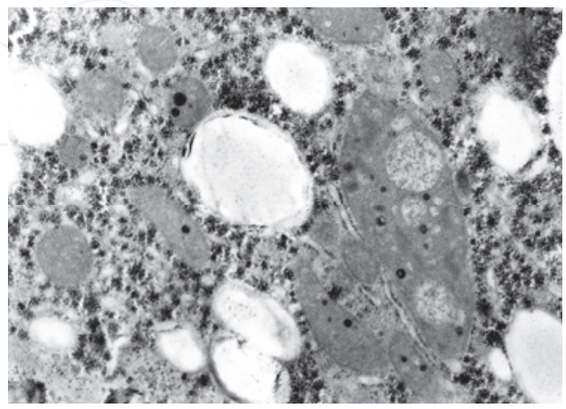

Fig. 45. Giant mitochondrion with punched-out areas and fat droplets. x 10,000

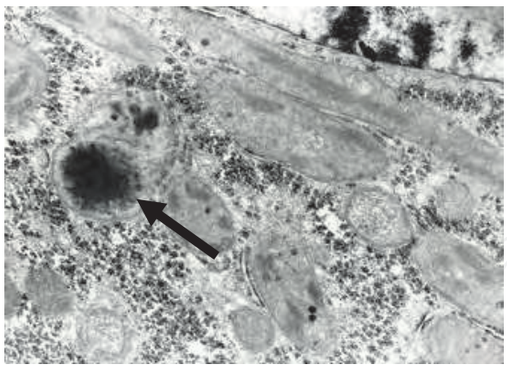

Fig. 46. WD: Mitochondria with crystalline deposits and dense deposits (arrow) x 8,000

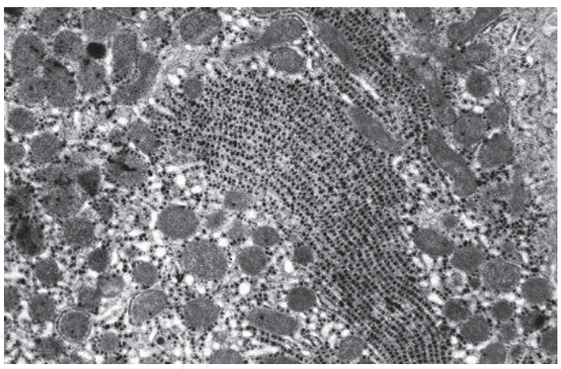

Fig. 47. Glycogen body (RER) frequently seen in WD. x 6,000

5.6 Reye syndrome

Around 1970, TEM had a major diagnostic role showing changes considered typical for Reye syndrome: generalized steatosis, glycogen depletion, increased frequency of peroxisomes and "amoeboid", occasionally giant mitochondria; their matrix was described as "flocculent" and frequently contained crystalline inclusions and lacked dense matrical granules (Figs. 48-49). Towards 1980, possibly following the reduced aspirin consumption, the frequency of Reye syndrome decreased dramatically. However, sporadic cases still occurred without a clear relationship to aspirin ingestion. The ultrastructural findings were similar to those described in Reye syndrome, and were therefore named "Reye-like" (Phillips et al., 1987). In the UK, over 10% of reported cases with an initial diagnosis of Reye's syndrome have later been revised to an *Inborn Metabolic Disorder (IMD)* which may mimic Reye's syndrome. IMD includes defects in fat oxidation, amino acid metabolism, carbohydrate metabolism and disorders of ammonia detoxification. The relationship with aspirin ingestion was not firmly established, as Reye syndrome appeared in areas where aspirin was never used (Australia) and continued to appear after aspirin was discontinued (France).

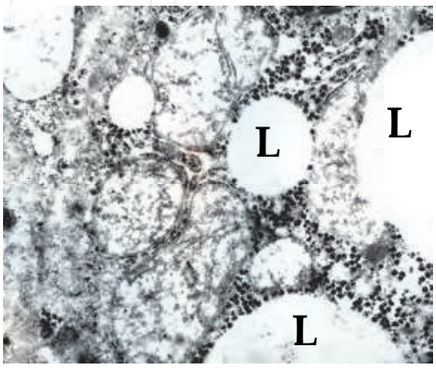

Fig. 48. Reye syndrome. Cristolysis and generalized lipid deposition (L) x 20,000

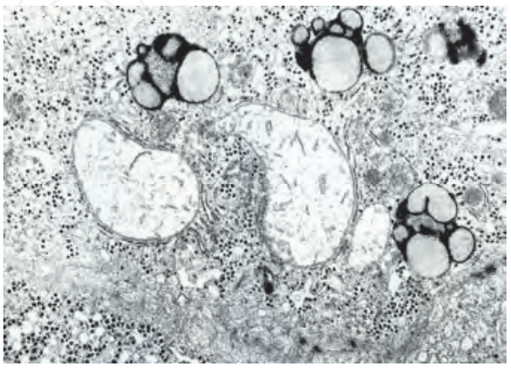

Fig. 49. Reye syndrome. Expanded mitochondria, cristolysis, lipofuscin and absent matrical granules. x 10,000

5.7 Steatosis

This group includes presently: 1. Alcoholic liver disease; 2. NAFLD (non-alcoholic fatty liver disease) which encompasses most forms of fatty liver, including "simple steatosis", without inflammation, seen in an important percent of adult population (Fig. 50), and 3. NASH, (non-alcoholic steatohepatitis) which by definition involves inflammation and/or fibrosis (Roberts, 2004 b) and may progress to cirrhosis more frequently than simple steatosis.

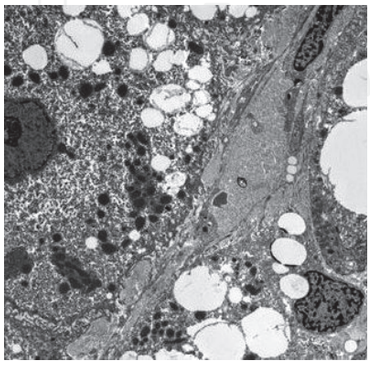

Fig. 50. Fatty liver - NAFLD: Large droplets present in hepatocytes and sinusoidal cells x 4,000

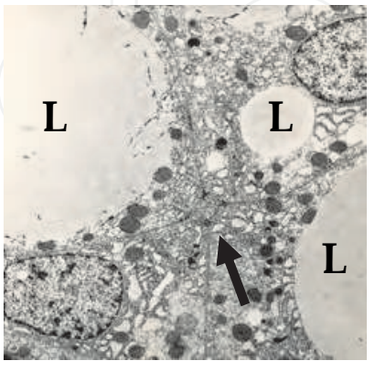

Fig. 51. Total parenteral nutrition. Lipid droplets (L) strangle a minute bile canaliculus (arrow). x 6,000

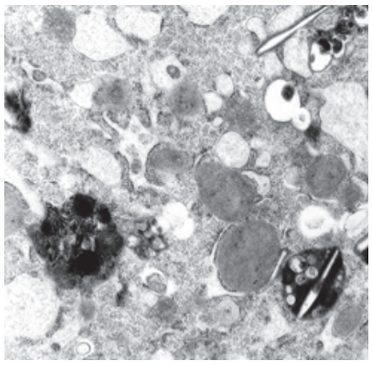

Fig. 52. Total parenteral nutrition. Spicular cholesterol within dense bodies. Abnormal mitochondria. x 8,000

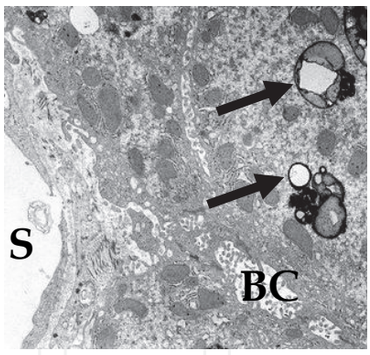

Fig. 53. NAFLD. Lipofuscin- lipolysosomes (arrows) near the sinusoid (S) and bile canaliculus (BC). x 4,000

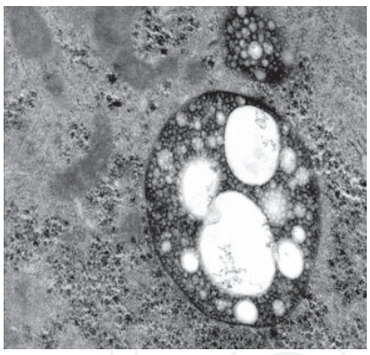

Fig. 54. Hepatocyte. Typical lipolysosomes, Wilson disease. x 6,000

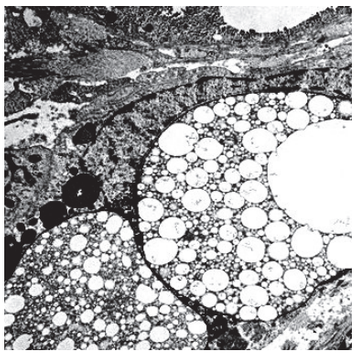

Fig. 55. Compound lipolysosome. Note extreme size compared to adjacent nuclei; x 6,000

For electron-microscopic characterization of liver steatosis, the classical terms "large droplet"(macrovesicular) and "small droplet"(microvesicular) are still used. Macrovesicular steatosis is mostly seen in nutritional abnormalities including: kwashiorkor, obesity, prolonged parenteral nutrition (Figs. 51-52), diabetes mellitus, glycogenoses, Wilson disease, hyperlipidemias, A-(or hypo) betalipoproteinemia, familial lipoprotein deficiency, total lipodystrophy (Sherlock & Doodley, 1993). Microvesicular steatosis is frequently found in mitochondrial dysfunctions, urea cycle enzyme defects, lysosomal storage diseases, Reye- and Reye-like syndromes, lipodystrophies and certain drug toxicities such as salicylates and valproate).

Fat droplets of various sizes can be seen mostly, but not only, in hepatocytes. The ubiquitous triglyceride droplets have a round contour, are only slightly electron dense and usually have no surrounding limit membrane. Even in cells apparently completely filled-up with fat droplets, the changes in other organelles are rare, with the exception of crystal formation in mitochondria, seen more frequently. Occasionally, a fat droplet can be seen in the nucleus as well.

5.7.1 Atypical lipid-containing organelles

Membrane-bound lipid droplets (lipolysosomes) are frequently seen in hepatocytes in association with triglyceride-containing droplets.

We distinguish between several types of lipid-containing, membrane-bound bodies:

1. *Lipolysosomes* as described by Hayashi and Sternlieb, and Kanai et al.(Hayashi & Sternlieb, 1975; Hayashi et al., 1983; Kanai et al., 1994). Electron-lucent droplets, usually up to 10 μm in diameter, with uniform content and surrounded by a trilaminar membrane. Of special interest are vesicles (attachments) to the outer leaflet of the surrounding membrane and associated lipofuscin (Figs. 53).
2. *Multivesicular bodies*, described by Phillips et al. (1987) as lipolysosomes, containing numerous smaller droplets with lipidic aspect (Fig. 54). Such lipolysosomes have been observed frequently in Wilson disease and in patients with NAFLD. They are frequently seen in hepatocytes showing increased amounts of typical lipofuscin
3. *Giant lipolysosomes* (Fig. 55) which we suggest to name "compound lipolysosomes", observed in cases of extreme overweight (Haimi et al., 2011). They appear to be formed by the fusion of numerous lipolysosomes of usual size, through a process similar to the formation of "compound siderosomes" describe in iron overload (Roy & Ghadially, 1967).

6. Infections and infestations (See Table 1)

Negative staining is required for identification of some viral particles while others display characteristic features in cytosol or nucleus in various liver cells. In acute hepatitis, remnants of *apoptotic* hepatocytes form eosinophilic *acidophilic bodies (Fig. 56).* They are then expelled from the cell aggregate and later phagocytized by macrophages. Other cells undergo necrosis without an identifiable apoptotic stage (Fig. 57).

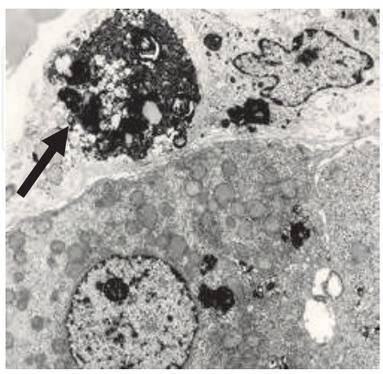

Fig. 56. Acidophilic body (arrow) in the sinusoid. Fat droplets, disintegrated nucleus and phagolysosomes are still recognizable. x 5,000

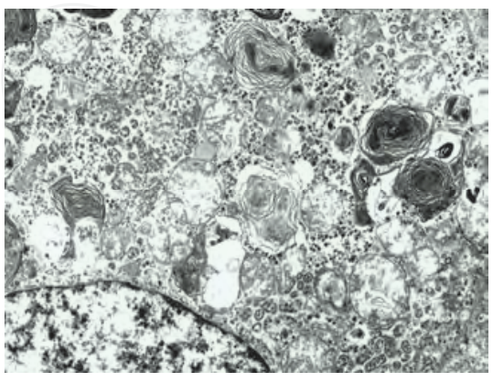

Fig. 57. Acute hepatitis: Membranous phagolysosomes in a necrotic hepatocyte. x 6,000

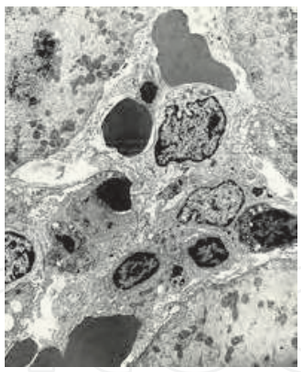

Fig. 58. Acute hepatitis. Mononuclear cells in sinusoid. x 4,000

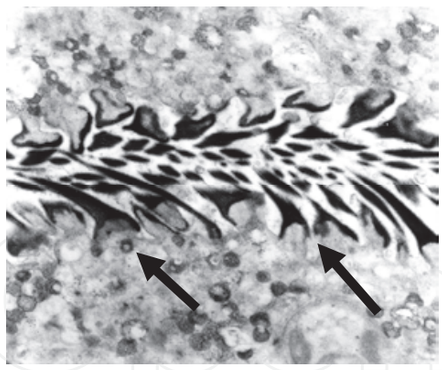

Fig. 59. Echinoccocus granulosum: hooklets (arrows) in the liver biopsy retrieved at surgery. x 10,000

The presence of inflammatory reactions, mostly of viral origin, is visualized by TEM initially by the presence of mononuclear cells in sinusoids (Fig. 58). Focal cytoplasmic degeneration precedes changes recognizable by light microscopy, to be followed by apoptosis and eventually necrosis. The identification of various hepatitis etiological agents is beyond the routine liver biopsy examination. The occasional encounter with parasites (Fig. 59) has an investigational character,

7. Drug hepatotoxicity

With the exponential increase in the number of drugs (medication) there is a parallel increase in the number of side- and toxic effects reported by patients. Many of these are related to liver function and metabolism and to the major de-toxifying role of this organ. In drug-induced damage, autophagosomes are frequently seen (Fig. 60) occasionally containing mitochondria (Fig. 61). In this review we will exemplify only a few of these toxic changes as seen by electron microscopy: non-specific effects, from mild and reversible to severe and life-endangering are listed in Table 1. In addition, there are some specific features which enable diagnosis of the offending compound: amiodarone, NSAIDs, aspirin, corticosteroids.

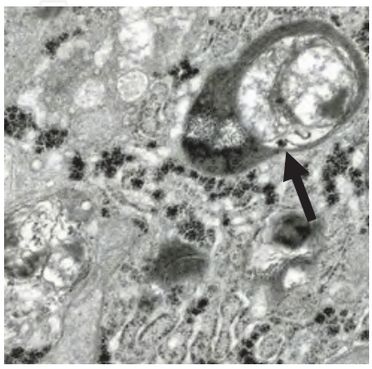

Fig. 60. Drug toxicity. Autophagosomes (arrows) contain fat and multiple membranes. x 15,000

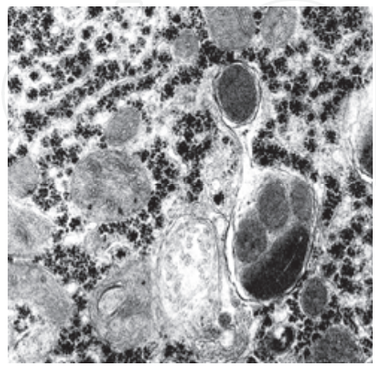

Fig. 61. Valproate toxicity. Mitochondria secluded in autophagolysosome. x 15,000

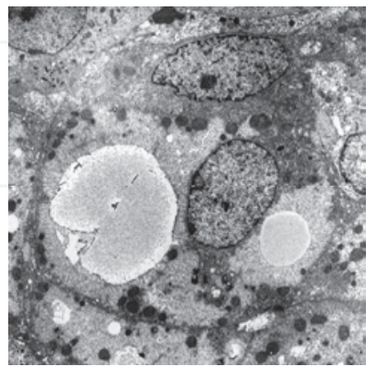

Fig. 62. Corticosteroid effect. Lipid and excessive glycogen in a bi-nucleated hepatocyte. x 6,000

Condition	EM findings
Artefacts	
Delayed fixation Inadequate fixation	Mitochondrial matrix with dense deposits 'Ballooned' mitochondria, 'Extraction' of nuclei Myelin-like whorls in mitochondria
Infections/ infestations	
Hepatitis, herpes-varicella group virus	viral particles
Hepatitis, acute (HBV)	viral particles (HBsAg) Nuclear Dane particles (HBcAg)
Infectious mononucleosis	Ebstein-Barr virus
Cytomegalovirus infection	Electron-dense particles in hepatocytes (no virus)
Kala-Azar	Leishmania bodies in Kupffer cells
Malaria	Schizonts in Kupffer cells
Ecchinococosis	Fragments in tissue
Bilirubin retention syndromes	
Unconjugated hyperbilirubinemia – Inherited disorders (Constitutional, non-hemolytic)	
Crigler-Najjar syndromes, type 1 & 2	Intracanalicular bile thrombi, increased intercellular space.
Gilbert's disease	Flattening of hepatocyte microvilli, reduced RER, proliferated SER.
Conjugated hyperbilirubinemia	
Cholangiopathies - Cholestasis (most etiologies)	Curled cristae in mitochondria; dense deposits in cell sap; amorphous and/or filamentous bile cytolysosomes mostly around bile canaliculi; focal biliary necrosis; dilated & distorted bile canaliculi with abnormal microvilli and bile plugs. Pericanalicular cytoplasm may show microfilaments.
Biliary atresia - Biliary duct obstruction	Extensive cytoplasmic cholestasis, cytoplasmic biliary necrosis; pericanalicular filamentous cuff.
Cystic fibrosis	Cholestasis in infancy; aggregates of osmiophilic material in lumen; collagen; steatosis; ductule dilatation; many stellate cells.
Alagille	Numerous bile-containing cytolysosomes and vesicles in Golgi; canaliculi can be empty.
PFIC 1 (ATP8B1)	Severe cholestasis (hepatocytes, sinusoidal cells, bile ducts, granular Byler bile).

PFIC 2 (ABCB11)	As in PFIC-1 but amorphous and filamentous bile in canaliculi.
PFIC 3 (ABCB4)	As in PFIC 1 & PFIC 2 but amorphous and filamentous bile in canaliculi.
Dubin-Johnson syndrome	Lipofuscin-like pigment, abnormal bile canaliculi.
Rotor syndrome	Megamitochondria, reduced microvilli in bile canaliculi.
Carbohydrate metabolism	
Glycogen Storage Diseases (GSD) Type I,(I-a) III, VI, VIII, IX, X, XI	Accumulation of cytosolic glycogen in hepatocytes; displacement of organelles; frayed α-glycogen in types VI, VIII, IX, X.
Type IIa, b, c	Abnormal glycogen-containing lysosomes: glycogenosomes.
Type IV (amilopectinosis)	Abnormal structural glycogen, collagen deposition and cirrhosis.
Diabetes mellitus	As for GSD I and III; micro- and macrovesicular steatosis. Hyperglycogenation of nuclei. Lipolysosomes, lipofuscin; mitochondrial crystalline inclusions.
Hereditary fructose intolerance	Concentric membranous arrays in hepatocytes; Areas of cytoplasmic damage: 'Fructose holes': abundant glycogen, prominent lipid droplets, large autophagic glycogen-containing vacuoles, myelin figures, focal cytoplasmic degradation.
Galactosemia	Hepatocytes: rosette or pseudoglandular formation; multinuclear hepatocytes. Cholestasis; large lipid droplets; distended RER
Disorders of glycoprotein metabolism	
Mucopolysaccharidoses : Hurler, Hunter, Sanfilippo, Scheie, Morquio, Maroteaux-Lamy	Abnormal lysosomes in hepatocytes, RER, sinusoidal cells and vascular epithelia; empty-looking vacuoles, occasional 'bull's eye' appearance.
Glycoproteinoses	
Fucosidosis	Lysosomes with variable membranous content.
Sialidosis (Mucolipidosis I)	Fine reticular-granular content of lysosomes (hepatocytes and sinusoidal cells).
Mannosidosis	Fine reticular-granular content of lysosomes. Electron-opaque globules in Kupffer cells.

Salla disease	"Empty lysosomes ": parenchymal & sinusoidal cells.
Glutamyl ribose 5-phosphate glycoproteinosis	Vacuoles with floccular material in Kupffer cells.
Mucolipidoses	
Mucolipidosis II (I-cell disease)	Cytoplasmic membrane- bound vacuoles containing fibrillose-granular material.
Mucolipidosis III (Pseudo-Hurler)	Vacuoles in cultured fibroblasts.
Mucolipidosis IV	Hepatocytes: lamellar inclusions; Kupffer cells: fibrogranular material in lysosomes.
Alpha-1-AT deficiency	Amorphous accumulations in hepatocytic RER.
Disorders of lipid metabolism	
Sphingolipidoses - Gangliosidoses	
GM1 (generalized gangliosidosis) Landing)	Membranous cytoplasmic bodies. Lipid-laden histiocytes (liver).
GM2 (Tay-Sachs, Sandhoff disease)	Membranous cytoplasmic bodies.
Glycosphingolipid lipidosis (Fabry disease)	Lysosomal concentric arrays disease.
Lactosyl ceramidosis	Lysosomal lamellae.
Sulphatidosis (metachromatic leukodystrophy)	Hepatocytic lamellar inclusions "Herring bone"
Glucocerebrosidosis (Gaucher disease)	Gaucher cells.
Ceramidosis (Farber disease)	Hepatocytic vacuoles and dense bodies; curved tubular structures in Kupffer cells.
Sphingomyelinosis (Niemann-Pick disease)	
(All types)	Lysosomal concentric membranes in hepatocytes and sinusoidal cells.
Abetalipoproteinemia	Macrovesicular liver steatosis. Deficient trans-Golgi vacuole formation
Familial lipoprotein deficiency	Lipolysosomes in foam cells of RES.
Acid lipase deficiency & Wolman disease	Foamy histiocytes containing acicular crystal lipid droplets in hepatocytes and histiocytes.
Cholesteryl ester storage disease	Cholesteryl ester crystals in Kupffer cells.
Ceroid lipofuscinosis	Lipofuscin and tubular structures in lysosomes.
Chanarin-Dorfman disease	Ichthyosis, fatty liver, cirrhosis.
Steroid therapy, prolonged	Macrovesicular liver steatosis.
Total lipodystrophy & Parenteral nutrition	Macrovesicular steatosis, lipid lakes, cholestasis
Disorders of protein metabolism	
Tyrosinemia	Cholestasis, steatosis, abnormal MV, collagen in space of Disse.

Aspartylglucoaminuria	Large lysosomes in hepatocytes &Kupffer cells. Membranous structures in mitochondria.
Carbamyl phosphate synthetase deficiency	Concentric RER, small mitochondria with high matrix density.
Lysinuric protein intolerance with deficient transport of basic amino acids	Increased SER; large vesicles filled with fibrogranular material.
Carnitine palmoyl transferase deficiency	Large-droplet fatty liver.
Hyperornithinemia	Megamitochondria, abnormal shapes and membranes.
Cystinosis	Crystals in Kupffer cell lysosomes.
Homocystinuria	Mitochondria abnormal shapes, SER. proliferation, peribiliary lysosomes.
Metals	
Iron	
Primary and secondary hemochromatosis	Ferritin in cytosol and lysosomes (siderosomes) Hemosiderin only in lysosomes (most cell lines)
Transfusional siderosis	RES hemosiderin loading, less in parenchyma.
Neonatal hemochromatosis Aceruloplasminemia	Heavy parenchymal siderosis, less in RES (distribution similar to hemochromatosis) Brain and systemic siderosis, including liver
Association with lipofuscin	Ferritin and hemosiderin in compound lysosomes with lipofuscin.
Copper	
Wilson disease	Abnormal mitochondria, abnormal peroxisomes, lipolysosomes, fatty liver, electron-dense deposits.
Menkes' kinky hair syndrome	Cartwheel-like cristae in mitochondria.
Peroxisomal disorders	
Zellweger syndrome	Absent peroxisomes.
Hepatic acatalasia syndrome	Absent peroxisomes.
Neonatal adrenoleukodystrophy	Few, small, peroxisomes.
Primary hyperoxaluria Type I	Few, small, peroxisomes
Infantile Refsum's disease	Few, small peroxisomes; angulated lysosomes.
Drug Toxicity – general features	Mitochondrial changes(absent dense matrical granules, paracrystalline formation); RER dilatation, SER proliferation; increased. frequency of lysosomes (autophagolysosomes); apoptosis, focal necrosis, lipofuscinosis.

Corticosteroid therapy, high dosage, short term	Glycogen accumulation in hepatocytes.
Miscellaneous	
Kwashiorkor, protein-calorie malnutrition	Large droplet fatty liver, abnormal mitochondria.
Chediak-Higashi disease	Abnormal inclusions in Kupffer cells and hepatocytes.
Erythrohepatic-protoporphyria	Amorphous or needle-like pigment in hepatocytes and Kupffer cells.
Erythroblastosis fetalis	Erythroblasts and reticulocytes in liver parenchyma.
GVH disease	Immune cell infiltrate.
Langerhans Cell Histiocytosis	Birbeck granules.
Parenteral nutrition	Mitochondrial changes, vesiculated SER, cholestasis, lipofuscin, in hepatocytes and Kupffer cells.
Reye syndrome & Reye-like syndrome	Microvesicular fatty liver, abnormal mitochondria, many peroxisomes.

Table 1. Electron Microscopic findings in different conditions

7.1 Corticosteroid effect

Fatty liver has been reported among the side-effects of prolonged large-dose steroid therapy (Sherlock & Doodley, 1993). Three patients aged 8, 10 and 12 year respectively, treated with medium-high doses of corticosteroids presented with hepatomegaly and elevated transaminases of unknown origin. Liver biopsy performed to elucidate these findings, revealed (by TEM) excessive glycogen in hepatocytes, to the extent of justifying hepatomegaly. The increased amount of hepatocytic glycogen displaced mitochondria and other components towards the nucleus and plasma membrane (Fig. 62). The pattern was similar to that of glycogen storage diseases observed in type III and IX. Lipid droplets were scarce. After the steroid therapy was discontinued, the liver size returned to normal (Iancu et al., 1986).

7.2 Amiodarone

Changes similar to alcoholic liver injury are commonly found. Steatosis, is the most frequent histopathological feature. Ballooning of hepatocytes, Mallory bodies, and fibrosis are common. Other changes include nuclear unrest, acidophilic bodies, foam cells, hyperglycogenated nuclei, and portal inflammation. Characteristic lamellar lysosomal inclusion bodies representing phospholipidosis should be better designed as "myelinosomes"(Fig. 63), (Ghadially, 1997). The cytotoxic pseudoalcoholic changes could be an independent phenomenon in susceptible patients unable to metabolize the drug. The true incidence of hepatic injury from amiodarone remains to be determined from prospective evaluations of pretreatment and follow-up liver biopsies (Lewis et al., 1990).

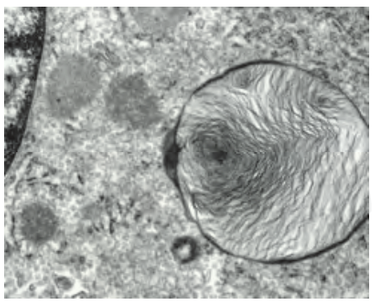

Fig. 63. Amiodarone toxicity: lamellar phosphor-lipidosis in a lysosome x 10,000

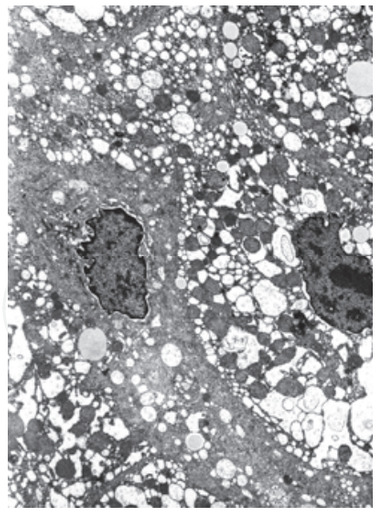

Fig. 64. Aspirin toxicity: dilated RER; steatosis, shrunken nuclei. x 4,000

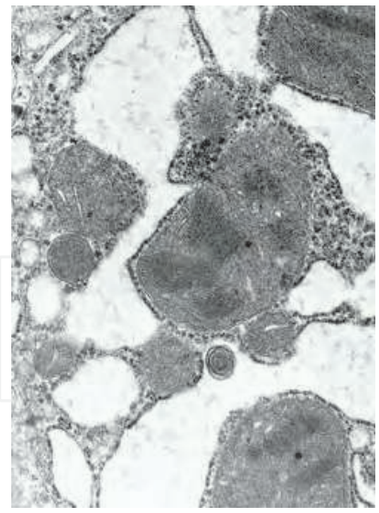

Fig. 65. Aspirin toxicity: dilatation of RER; crystalline deposits. x 10,000

7.3 Acetylsalicylic acid (Aspirin)

In addition to its suspected relationship to Reye syndrome, aspirin, in large doses, has been found to increase the level of transaminases, a reversible reaction. TEM of a liver biopsy of a patient disclosed hepatotoxicity: dilatation of RER, mitochondrial changes (megamitochondria, crystalline formation), nuclear changes and lipofuscinosis (Figs. 64-65), (Iancu & Elian, 1976).

7.4 Acetaminophen (Paracetamol)

Frequently used as a suicidal drug, paracetamol can precipitate fatal liver failure when dosage is beyond 8–10g. TEM of experimental animals and cultured hepatoma-derived cells (HepG2 and Hep3B) disclosed the different stages of dose-related toxicity. Of note, the anti-oxidant *N*-acetylcysteine did not protect cultured cells against acetaminophen-induced apoptosis (Manov et al., 2002; Manov et al., 2004). Various aspects of ultrastructural damage induced by non-steroidal anti-inflammatory drugs (NSAIDs) are described in detail in a review of hepatotoxicity of anti-inflammatory and analgesic drugs (Manov et al., 2006).

8. Conclusions

Transmission electron microscopy of liver biopsies provides:

1. **Typical diagnostic findings** for a relatively small, but important, number of pathological conditions.
2. **Supportive information** for a larger group of suspected conditions which require further confirmation.
3. **Important exclusion** of conditions which were considered in differential diagnosis.

Furthermore, it remains an essential research tool in all areas of bio-pathology.

9. Acknowledgments

The electron-microscopic work was supported by The Milman Fund for Pediatric Research and the Dan David Foundation (Grant 03-06, 2010) and by a joint grant to Dr. I. Manov from The Center of Absorption in Science of the Ministry of Immigrant Absorption and the Committee for Planning and Budgeting of the Council for Higher Education, in the framework of the Kamea Program.
The following colleagues submitted liver specimens for examination: D. Berkowitz, H. Bitterman, J. Bujanover, D. Bransky, E. Broide, I. Dalal, M. Haimi, C. Hartman A. Lerner, A. Levine, H. Mandel, A. On, A. Pecht, S. Peleg, H. Shamali, R. Shaoul, R. Shamir, R. Shapiro, R. Spiegel, R. Regev, M. Wilschanski, N. Zelnick, E. Zuckerman.

10. References

Balistreri, W. F. (2002). Intrahepatic cholestasis. *J Pediatr Gastroenterol Nutr*, Vol. 35 Suppl 1, No. S17-23

Bessis, M. & Weed, R. I. (1973). *Living blood cells and their ultrastructure. Translated [and edited] by Robert I. Weed,* Springer-Verlag, New York,

Bezerra, J. A. & Balistreri, W. F. (1999). Intrahepatic cholestasis: order out of chaos. *Gastroenterology*, Vol. 117, No. 6, 1496-8

Bull, L. N.; Carlton, V. E.; Stricker, N. L.; Baharloo, S.; DeYoung, J. A.; Freimer, N. B.; Magid, M. S.; Kahn, E.; Markowitz, J.; DiCarlo, F. J.; McLoughlin, L.; Boyle, J. T.; Dahms, B. B.; Faught, P. R.; Fitzgerald, J. F.; Piccoli, D. A.; Witzleben, C. L.; O'Connell, N. C.; Setchell, K. D.; Agostini, R. M., Jr.; Kocoshis, S. A.; Reyes, J. & Knisely, A. S. (1997). Genetic and morphological findings in progressive familial intrahepatic cholestasis (Byler disease [PFIC-1] and Byler syndrome): evidence for heterogeneity. *Hepatology*, Vol. 26, No. 1, 155-64

Davit-Spraul, A.; Gonzales, E.; Baussan, C. & Jacquemin, E. (2009). Progressive familial intrahepatic cholestasis. *Orphanet J Rare Dis*, Vol. 4, No. 1

Fischbach, F. A.; Gregory, D. W.; Harrison, P. M.; Hoy, T. G. & Williams, J. M. (1971). On the structure of hemosiderin and its relationship to ferritin. *J Ultrastruct Res*, Vol. 37, No. 5, 495-503

Gal, S.; Fridkin, M.; Amit, T.; Zheng, H. & Youdim, M. B. (2006). M30, a novel multifunctional neuroprotective drug with potent iron chelating and brain selective monoamine oxidase-ab inhibitory activity for Parkinson's disease. *J Neural Transm Suppl*, Vol. No. 70, 447-56

Ghadially, F. N. (1997). *Ultrastructural pathology of the cell and matrix,* Butterworth-Heinemann, Boston

Hackenbrock, C. R.; Rehn, T. G.; Weinbach, E. C. & Lemasters, J. J. (1971). Oxidative phosphorylation and ultrastructural transformation in mitochondria in the intact ascites tumor cell. *J Cell Biol*, Vol. 51, No. 1, 123-37

Hayashi, H.; Sameshima, Y.; Lee, M.; Hotta, Y. & Kosaka, T. (1983). Lipolysosomes in human hepatocytes: their increase in number associated with serum level of cholesterol in chronic liver diseases. *Hepatology*, Vol. 3, No. 2, 221-5

Hayashi, H. & Sternlieb, I. (1975). Lipolysosomes in human hepatocytes. Ultrastructural and cytochemical studies of patients with Wilson's disease. *Lab Invest*, Vol. 33, No. 1, 1-7

Hers, H. G. (1963). alpha-Glucosidase deficiency in generalized glycogenstorage disease (Pompe's disease). *Biochem J*, Vol. 86, No. 11-6

Iancu, T. & Elian, E. (1976). Ultrastructural changes in aspirin hepatotoxicity. *Am J Clin Pathol*, Vol. 66, No. 3, 570-5

Iancu, T. C. (1983). Iron overload. *Mol Aspects Med*, Vol. 6, No. 1, 1-100

Iancu, T. C. (1989). Ultrastructural pathology of iron overload. *Baillieres Clin Haematol*, Vol. 2, No. 2, 475-95

Iancu, T. C. (1992). Ferritin and hemosiderin in pathological tissues. *Electron Microsc Rev*, Vol. 5, No. 2, 209-29

Iancu, T. C. (2011). Ultrastructural aspects of iron storage, transport and metabolism. *Journal of neural transmission (Vienna, Austria : 1996)*, Vol. No.

Iancu, T. C.; Deugnier, Y.; Halliday, J. W.; Powell, L. W. & Brissot, P. (1997). Ultrastructural sequences during liver iron overload in genetic hemochromatosis. *J Hepatol*, Vol. 27, No. 4, 628-38

Iancu, T. C.; Mahajnah, M.; Manov, I.; Cherurg, S.; Knopf, C. & Mandel, H. (2007). The liver in congenital disorders of glycosylation: ultrastructural features. *Ultrastruct Pathol*, Vol. 31, No. 3, 189-97

Iancu, T. C.; Shiloh, H. & Dembo, L. (1986). Hepatomegaly following short-term high-dose steroid therapy. *J Pediatr Gastroenterol Nutr*, Vol. 5, No. 1, 41-6

Johannessen, J. V. (1978). *Electron microscopy in human medicine,* McGraw-Hill International Book Co., New York

Kanai, M.; Watari, N.; Soji, T. & Sugawara, E. (1994). Formation and accumulation of lipolysosomes in developing chick hepatocytes. *Cell Tissue Res*, Vol. 275, No. 1, 125-32

Knisely, A. S. & Vergani, D. "Neonatal hemochromatosis": a re-vision. *Hepatology*, Vol. 51, No. 6, 1888-90

Lewis, J. H.; Mullick, F.; Ishak, K. G.; Ranard, R. C.; Ragsdale, B.; Perse, R. M.; Rusnock, E. J.; Wolke, A.; Benjamin, S. B.; Seeff, L. B. & et al. (1990). Histopathologic analysis of suspected amiodarone hepatotoxicity. *Hum Pathol*, Vol. 21, No. 1, 59-67

Mandel, H.; Hartman, C.; Berkowitz, D.; Elpeleg, O. N.; Manov, I. & Iancu, T. C. (2001). The hepatic mitochondrial DNA depletion syndrome: ultrastructural changes in liver biopsies. *Hepatology*, Vol. 34, No. 4 Pt 1, 776-84

Manov, I.; Hirsh, M. & Iancu, T. C. (2002). Acetaminophen hepatotoxicity and mechanisms of its protection by N-acetylcysteine: a study of Hep3B cells. *Exp Toxicol Pathol*, Vol. 53, No. 6, 489-500

Manov, I.; Hirsh, M. & Iancu, T. C. (2004). N-acetylcysteine does not protect HepG2 cells against acetaminophen-induced apoptosis. *Basic Clin Pharmacol Toxicol*, Vol. 94, No. 5, 213-25

Manov, I.; Motanis, H.; Frumin, I. & Iancu, T. C. (2006). Hepatotoxicity of anti-inflammatory and analgesic drugs: ultrastructural aspects. *Acta Pharmacologica Sinica*, Vol. 27, No. 259-272

McAdams, A. J.; Hug, G. & Bove, K. E. (1974). Glycogen storage disease, types I to X: criteria for morphologic diagnosis. *Hum Pathol*, Vol. 5, No. 4, 463-87

Meiner, V.; Shpitzen, S.; Mandel, H.; Klar, A.; Ben-Neriah, Z.; Zlotogora, J.; Sagi, M.; Lossos, A.; Bargal, R.; Sury, V.; Carmi, R.; Leitersdorf, E. & Zeigler, M. (2001). Clinical-biochemical correlation in molecularly characterized patients with Niemann-Pick type C. *Genet Med*, Vol. 3, No. 5, 343-8

Mowat, A. P. (1994). *Liver disorders in childhood,* Butterworth-Heinemann, Oxford

Muir, W. A.; McLaren, G. D.; Braun, W. & Askari, A. (1984). Evidence for heterogeneity in hereditary hemochromatosis. Evaluation of 174 persons in nine families. *Am J Med*, Vol. 76, No. 5, 806-14

Partin, J. C.; Schubert, W. K. & Partin, J. S. (1971). Mitochondrial ultrastructure in Reye's syndrome (encephalopathy and fatty degeneration of the viscera). *N Engl J Med*, Vol. 285, No. 24, 1339-43

Pastores, G. M. (2010). *Lysosomal storage disorders : principles and practice,* World Scientific, Singapore

Spiegel, R.; Raas-Rothschild, A.; Reish, O.; Regev, M.; Meiner, V.; Bargal, R.; Sury, V.; Meir, K.; Nadjari, M.; Hermann, G.; Iancu, T. C.; Shalev, S. A. & Zeigler, M. (2009). The clinical spectrum of fetal Niemann-Pick type C. *Am J Med Genet A*, Vol. 149A, No. 3, 446-50

Sternlieb, I. (1979). Electron Microscopy of Mitochondria and Peroxysomes of Human Hepatocytes, In: *Progress in Liver Diseases*, P. Hans and S. Fenton, (Ed.), 81-104, Grune & Stratton, New York

Tandler, B.; Hutter, R. V. & Erlandson, R. A. (1970). Ultrastructure of oncocytoma of the parotid gland. *Lab Invest*, Vol. 23, No. 6, 567-80

Tanikawa, K.; Eguchi, T. & Ikejiri, N. (1979). *Ultrastructural aspects of the liver and its disorders,* Igaku-Shoin, Tokyo ; New York

Valencia-Mayoral, P.; Weber, J.; Cutz, E.; Edwards, V. D. & Phillips, M. J. (1984). Possible defect in the bile secretory apparatus in arteriohepatic dysplasia (Alagille's syndrome): a review with observations on the ultrastructure of liver. *Hepatology*, Vol. 4, No. 4, 691-8

Verhulst, P. M.; van der Velden, L. M.; Oorschot, V.; van Faassen, E. E.; Klumperman, J.; Houwen, R. H.; Pomorski, T. G.; Holthuis, J. C. & Klomp, L. W. A flippase-independent function of ATP8B1, the protein affected in familial intrahepatic cholestasis type 1, is required for apical protein expression and microvillus formation in polarized epithelial cells. *Hepatology*, Vol. 51, No. 6, 2049-60

Weber, A. M.; Tuchweber, B.; Yousef, I.; Brochu, P.; Turgeon, C.; Gabbiani, G.; Morin, C. L. & Roy, C. C. (1981). Severe familial cholestasis in North American Indian children: a clinical model of microfilament dysfunction? *Gastroenterology*, Vol. 81, No. 4, 653-62

Whitington, P. F. (2007). Neonatal hemochromatosis: a congenital alloimmune hepatitis. *Semin Liver Dis*, Vol. 27, No. 3, 243-50

Zhu, W.; Xie, W.; Pan, T.; Xu, P.; Fridkin, M.; Zheng, H.; Jankovic, J.; Youdim, M. B. & Le, W. (2007). Prevention and restoration of lactacystin-induced nigrostriatal dopamine neuron degeneration by novel brain-permeable iron chelators. *Faseb J*, Vol. 21, No. 14, 3835-44

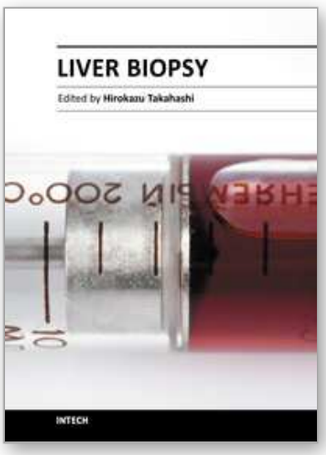

Liver Biopsy

Edited by Dr Hirokazu Takahashi

ISBN 978-953-307-644-7

Hard cover, 404 pages

Publisher InTech

Published online 06, September, 2011

Published in print edition September, 2011

Liver biopsy is recommended as the gold standard method to determine diagnosis, fibrosis staging, prognosis and therapeutic indications in patients with chronic liver disease. However, liver biopsy is an invasive procedure with a risk of complications which can be serious. This book provides the management of the complications in liver biopsy. Additionally, this book provides also the references for the new technology of liver biopsy including the non-invasive elastography, imaging methods and blood panels which could be the alternatives to liver biopsy. The non-invasive methods, especially the elastography, which is the new procedure in hot topics, which were frequently reported in these years. In this book, the professionals of elastography show the mechanism, availability and how to use this technology in a clinical field of elastography. The comprehension of elastography could be a great help for better dealing and for understanding of liver biopsy.

INTECH
open science | open minds

InTech Europe
University Campus STeP Ri
Slavka Krautzeka 83/A
51000 Rijeka, Croatia
Phone: +385 (51) 770 447
Fax: +385 (51) 686 166
www.intechopen.com

InTech China
Unit 405, Office Block, Hotel Equatorial Shanghai
No.65, Yan An Road (West), Shanghai, 200040, China
中国上海市延安西路65号上海国际贵都大饭店办公楼405单元
Phone: +86-21-62489820
Fax: +86-21-62489821

IntechOpen